Findings of Extrathyroid Lesions Encountered With Thyroid Sonography

Jin Young Kwak, MD, Eun-Kyung Kim, MD, Sun Young Park, MD, Min Jung Kim, MD, Won-Jin Moon, MD, Seon Hyeong Choi, MD, Eun Ju Son, MD, Ki Keun Oh, MD, Ki Whang Kim, MD, Woo-Ick Yang, MD, Ju Yeon Pyo, MD

Objective. The purpose of this presentation is to illustrate the normal sonographic anatomy of the anterior neck region and the sonographic findings of various kinds of extrathyroid lesions. ***Methods.*** Cases of extrathyroid lesions were collected and reviewed retrospectively from our archives. All of the sonographic examinations were performed with high-frequency (5- to 15-MHz) linear array transducers. ***Results.*** The normal sonographic anatomy of the anterior neck region and various pathologic conditions of patients with extrathyroid lesions are discussed. ***Conclusions.*** Sonography is a useful imaging method for evaluating anterior neck anatomy and various pathologic conditions in patients with extrathyroid lesions. ***Key words:*** neck anatomy; sonography; thyroid glands.

Abbreviations
CT, computed tomography; H&E, hematoxylin-eosin; MRI, magnetic resonance imaging

Received July 9, 2007, from the Department of Diagnostic Radiology (J.Y.K., E.-K.K., M.J.K., S.H.C., E.J.S., K.K.O., K.W.K.), Research Institute of Radiological Science (J.Y.K., E.-K.K., M.J.K., S.H.C., E.J.S., K.K.O., K.W.K.), and Department of Pathology (W.-I.Y., J.Y.P.), Yonsei University College of Medicine, Seoul, Korea; Gachon University Gil Medical Center, Incheon, Korea (S.Y.P.); and Konkuk University, Seoul, Korea (W.-J.M.). Revision requested July 26, 2007. Revised manuscript accepted for publication September 6, 2007.

Address correspondence to Eun-Kyung Kim, MD, Department of Diagnostic Radiology, Yonsei University College of Medicine, 250 Seongsanno, 134 Sinchon-dong, Seodaemun-gu, Seoul 120-752, Korea.

E-mail: ekkim@yumc.yonsei.ac.kr

With the increased use of state-of-the-art sonography, many anterior neck lesions, including thyroid lesions, are being found. Sonography of the neck is extremely sensitive in detecting thyroid and parathyroid lesions, cervical lymph nodes, and other neck lesions,[1] although some parathyroid lesions with an ectopic location can be missed by sonography. The high sensitivity of sonography is due to the superficial locations of most structures within the anterior neck and superior sonographic imaging provided by small parts transducers with frequencies of 7.5 to 15 MHz.

This presentation discusses and illustrates many extrathyroid lesions mimicking thyroidal lesions. These case examples provide a framework for sharing interpretative pearls and pitfalls with practicing radiologists. Careful sonographic examination, along with knowledge of the anatomy of the cervical region, is very helpful in the diagnosis and differentiation of extrathyroid lesions.

Materials and Methods

The teaching files of our institution were searched. We retrospectively reviewed medical records and their associated sonographic features. All sonographic examinations were performed with a 7- to 15-MHz linear array transducer (HDI 5000; Philips Medical Systems, Bothell, WA), an 8- to 15-MHz linear array transducer (Acuson Sequoia; Siemens Medical Solutions USA, Inc, Mountain View, CA), or a 5- to 12-MHz linear array transducer (iU22; Philips Medical Systems). With the use of the HDI 5000 and iU22 machines, compound imaging was performed in all cases.

Sonographic Findings

Normal Anatomy

The anterior neck consists of a central visceral space and surrounding vascular, nervous, and muscular structures (Figure 1). The central visceral space includes the thyroid gland, parathyroid glands, cervical trachea or esophagus, recurrent laryngeal nerve, and paratracheal, prelaryngeal, and pretracheal lymph node groups.[1] Various diseases originating from organs in the visceral space can make differentiation of thyroid lesions difficult.

Parathyroid Diseases

The location of the parathyroid glands is variable. Humans usually have 4 parathyroid glands. The superior parathyroid glands are located at the posterior portion of thyroid gland at the level of upper or mid pole of the thyroid gland.[1,2] The location of inferior parathyroid glands is more variable. However, they are usually seen at the inferoposterior portion of the thyroid gland.[1,2] Normal parathyroid glands are not typically seen with sonography. However, pathologic parathyroid glands can be seen with sonography. Typically, parathyroid adenoma appears as a well-circumscribed round or oval hypoechoic nodule (Figure 2).[2] Parathyroid adenoma is the most common cause of primary hyperparathyroidism. Reeder et al[3] reported the characteristic imaging features and a systemic scanning approach for localization of parathyroid adenomas in patients with primary hyperparathyroidism. They suggested that several color Doppler features, including peripheral and polar vascularity, an enlarging feeding artery, and vascular asymmetry from localized hyperemia, could be useful for identifying parathyroid adenoma.[3] However, several structures such as lymph nodes, multinodular goiters, and other tumors found within the visceral space may mimic parathyroid adenoma. Infrequently, parathyroid adenoma may have cystic degeneration (Figure 3) and contain calcifications.[2] Parathyroid cysts are uncommon but when present are most commonly located below the inferior thyroid border. On sonography, a parathyroid cyst usually appears as a simple cyst with a prominent and thin wall (Figure 4). With fine-needle aspiration, there is a high level of parathyroid hormone within clear fluid.

Figure 1. Normal anatomy of the anterior neck on a transverse scan.

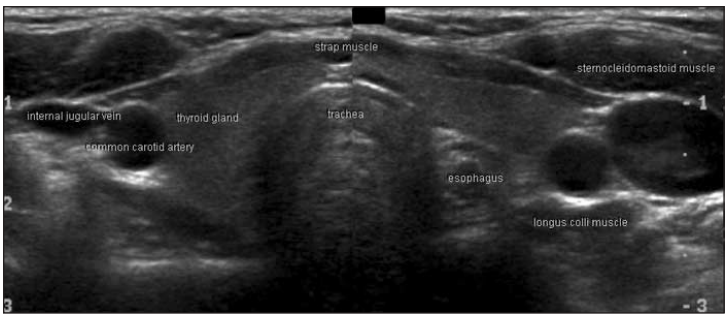

Central Lymph Nodes

Lymphatic tissue is abundant in the neck. Within the visceral space, many level VI lymph nodes exist. Most reactive lymph nodes can be easily differentiated from other masses because of an internal hyperechoic fatty hilum on sonography (Figure 5). However, pathologic central lymph nodes can be difficult to differentiate from other masses such as parathyroid lesions. Various diseases such as metastasis, lymphoma, and other benign conditions can manifest as pathologic lymph nodes at the central area. Metastatic lymph nodes (Figure 6) from papillary thyroid carcinoma can show cystic changes, hyperechoic punctuations, and loss of the hilum.[4] Reeder et al[3] suggested that color Doppler imaging could be useful for distinguishing between parathyroid adenoma and pathologic lymph nodes because the polar vascularity seen with parathyroid ade-

noma differed from the typical central hilar flow pattern seen with lymph nodes.

Hypopharyngeal or Esophageal Lesions

A pharyngoesophageal diverticulum is usually found incidentally during esophagography.[5] A pharyngoesophageal diverticulum occurs at sites of anatomic weakness in the hypopharynx or in the cervical esophagus near the cricopharyngeus muscle.[6] With the increased use of high-frequency sonography in evaluation of the neck, a pharyngoesophageal diverticulum can be initially detected on neck sonography. Because a pharyngoesophageal diverticulum contains air, this lesion can be misdiagnosed as a thyroid nodule with calcifications. However, trapped air within a pharyngoesophageal diverticulum can produce echogenic foci with a comet or reverberation artifact, which can help in differentiating a pharyngoesophageal diverticulum from a thyroid nodule with calcifciations.[7] A few reports have described several sonographic features for differentiating thyroid nodules from pharyngoesophageal diverticula.[7,8] These fea-

Figure 2. Parathyroid adenoma in a 63-year-old woman. **A** and **B**, Transverse and longitudinal gray scale sonograms show a well-defined hypoechoic mass (arrows) at the posterior aspect of the right thyroid gland. **C**, Technetium Tc 99m methoxy isobutyl isonitrile scan shows delayed wash-out (arrow) of the parathyroid adenoma. **D**, Pathologic specimen shows that the tumor is round to oval with a thin capsule (arrows). It shows a trabecular growth pattern of a mixture of chief cells and oncocytic cells (hematoxylin-eosin [H&E], original magnification ×12.5).

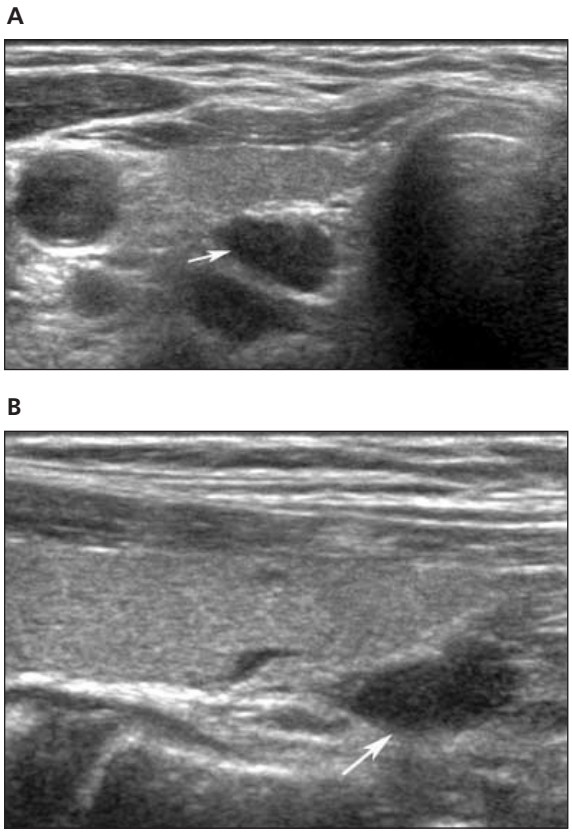

Figure 3. Parathyroid adenoma in a 42-year-old woman. **A** and **B**, Transverse and longitudinal gray scale sonograms show a well-defined hypoechoic mass (black arrows) with internal cystic degeneration (white arrows) at the posterior aspect of the thyroid gland. **C**, Pathologic specimen shows that the tumor is composed mainly of chief cells and shows dilated vasculature with a cystic lesion (arrows; H&E, original magnification ×12.5).

A

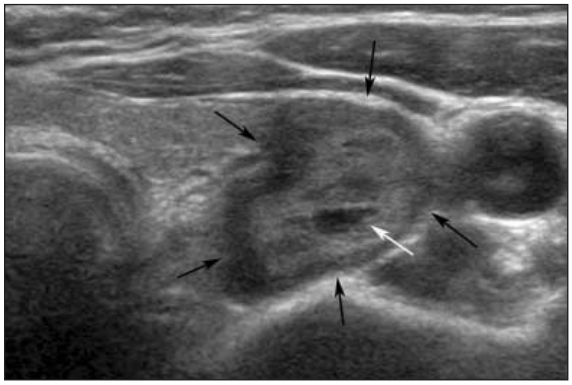

B

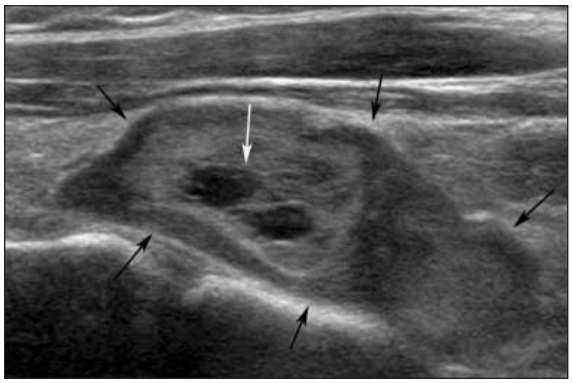

C

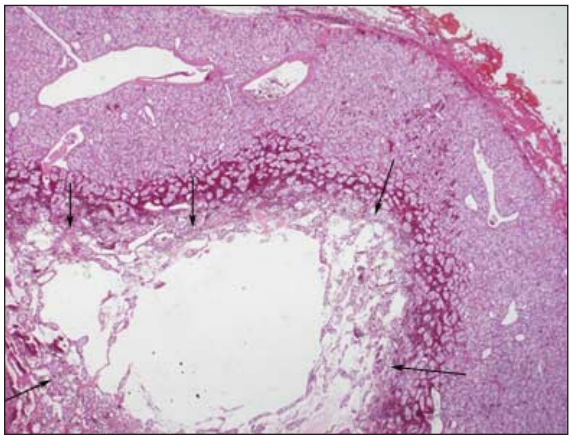

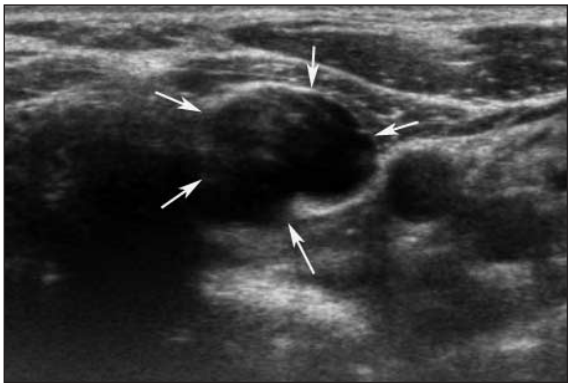

A

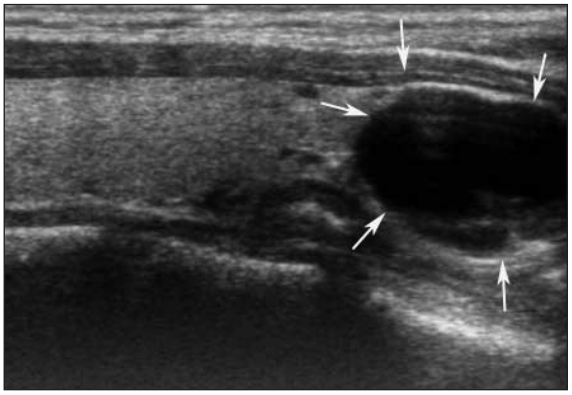

B

Figure 4. Parathyroid cyst in a 44-year-old woman. **A** and **B**, Transverse and longitudinal gray scale sonograms show a cyst with a thin wall (arrows) at the posterior aspect of the thyroid gland. At fine-needle aspiration, there was a high level of parathyroid hormone (762 ng/mL) within clear fluid.

Figure 5. Reactive lymph node (arrows) with an internal echogenic fatty hilum.

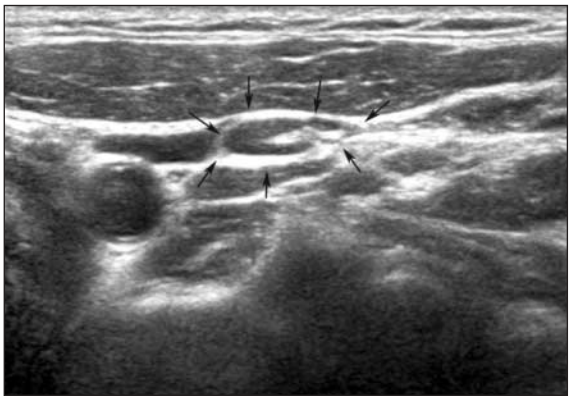

tures are as follows: first, there are changes in the shape and shadowing of the internal echoes that are associated with content changes in the diverticulum during swallowing; second, there is a connection to the esophagus (Figure 7); and last, there is a peripheral echogenic line or a boundary hypoechoic zone that is suggestive of the stratal structure of the digestive tract (Figure 7).[5,7–11]

Figure 6. Metastatic lymph node from papillary thyroid carcinoma in a 48-year-old man. **A** and **B**, Transverse and longitudinal gray scale sonograms show an oval mass with internal microcalcifications (black arrows) and cystic changes (white arrows) at the inferior aspect of the right thyroid gland. **C**, Pathologic specimen shows that the normal structure of the lymph node is distorted by tumor cells. Psammoma bodies are noted (arrows; H&E, original magnification ×40).

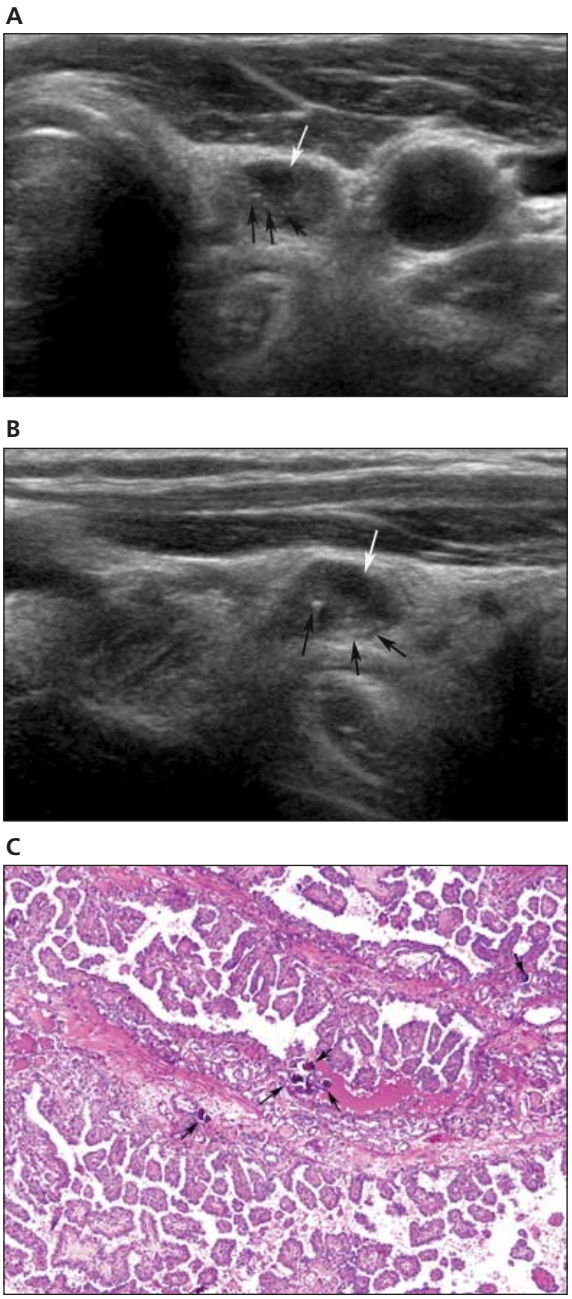

Figure 7. Pharyngoesophageal diverticulum in a 72-year-old man. **A**, Transverse gray scale sonogram shows a hypoechoic mass with internal echogenic spots (arrows) at the posterior aspect of the thyroid gland. **B**, Longitudinal gray scale sonogram shows a hypoechoic mass with a peripheral hypoechoic boundary and a connection to the esophageal wall (arrows). **C**, Esophagography confirms a Zenker diverticulum projecting to the left of the esophagus (arrow).

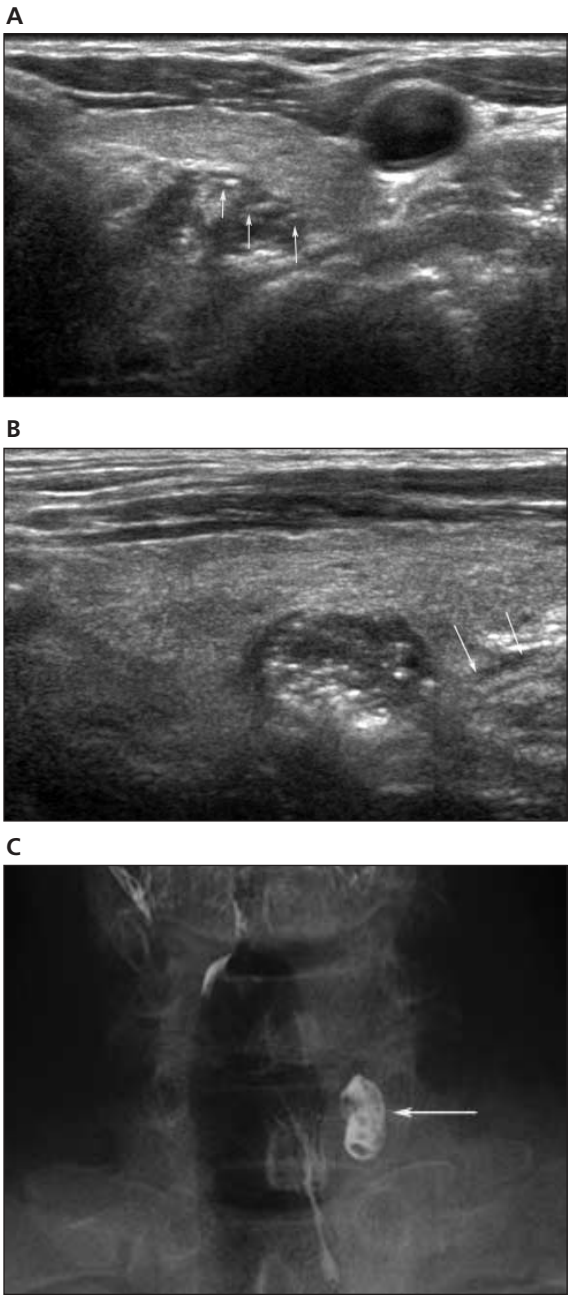

Esophageal carcinoma constitutes only about 1% of all cancers and 7% of cancers in the gastrointestinal tract.[12] For detection of esophageal malignancy, including early esophageal cancer, double-contrast esophagography has been widely accepted as the best diagnostic technique. Sonographic examination of the hypopharyngeal and cervical esophagus can be difficult. Therefore, sonograms are not routinely used to evaluate hypopharyngeal or esophageal cancer. Anatomically, the hypopharynx and esophagus are located near the posterior portion of the thyroid gland. Therefore, a mass originating from the hypopharynx and esophagus can be misinterpreted as a thyroid mass (Figure 8). When evaluating the neck node status for staging of hypopharyngeal or esophageal malignancy without the patient's history, the possibility of misdiagnosing the malignancy as thyroid in origin exists.

Tracheal Lesions

The extrathoracic trachea is encased anterolaterally by the thyroid gland. Therefore, tracheal masses can be found on sonographic evaluations of the neck. The most common tracheal tumor in adults is squamous cell carcinoma, followed by adenoid cystic carcinoma.[13] Squamous cell carcinoma is seen as focal or circumferential irregular thickening of the tracheal wall with luminal narrowing. In contrast to this, adenoid cystic carcinoma is a low-grade malignancy that tends to insidiously invade into the submucosal plane of the trachea. Adenoid cystic carcinoma is seen as either a broad-based or pedunculated polypoid lesion. It may show smooth or nodular thickening of the tracheal wall (Figure 9) with associated luminal narrowing.

Paratracheal air cysts are rare lesions, which are histologically lined by ciliated columnar epithelia and communicate with the trachea.[14–17] Most of them are located at the right posterolateral aspect of the trachea and are easily found by computed tomography (CT).[14,15] When sonography of the neck is performed, a paratracheal air cyst can be misdiagnosed as a parathyroid or thyroid mass.[18] The reported sonographic feature of a paratracheal air cyst is a masslike lesion containing hyperechoic foci at the right inferoposterior aspect of the thyroid gland and to the right of the trachea (Figure 10).[18] Internal hyperechoic foci within a paratracheal air cyst on sonography were due to air, which was proved by a phantom model by Kim et al.[18] Unlike pharyngoesophageal diverticula, there are no chronologic changes during swallowing.

Mediastinal Lesions

Many kinds of masses can arise in the prevascular space of the anterior mediastinum. These include thymic masses, germ cell tumors, lymphoma, thyroid masses, parathyroid masses, and other growths. Occasionally, a mediastinal mass can initially present as a cervical mass.[19–21] A mass originating from the superior mediastinum may extend superiorly into the thyroid space (Figures 11 and 12), just as a thyroid mass such as a goiter may extend inferiorly through the thoracic inlet into the superior mediastinum. On sonography, differentiation of these two lesions can be difficult, therefore needing additional imaging studies such as CT or magnetic resonance imaging (MRI). Among various mediastinal masses, teratoma can be easily diagnosed on CT or MRI when the mass has a fat component.[22] Therefore, the possibility of a mediastinal mass should be considered when the inferior margin of a cervical mass cannot be evaluated by real-time sonography.

Other Extrathyroid Lesions Originating From Surrounding Structures

Soft tissue fibromatosis can be divided into superficial and deep lesions. Desmoid tumors (deep fibromatosis) arise from musculoaponeurotic structures of the limb, neck, trunk, abdominal wall, and mesentery.[23] Desmoid tumors invade contiguous tissues and are most common between 25 and 35 years but can occur at any age.[23] The lesion is typically firm or hard and usually painless. Most neck desmoids are found in the upper neck (Figure 13). The tumor may be difficult to manage because of involvement of the great vessels, trachea, and brachial plexus. Surgery is the treatment of choice.

Peripheral nerve sheath tumors in the neck are relatively rare. The most common types are schwannoma and neurofibroma, which can be seen as a hypoechoic mass with distal acoustic enhancement on sonography (Figure 14).[24]

A

B

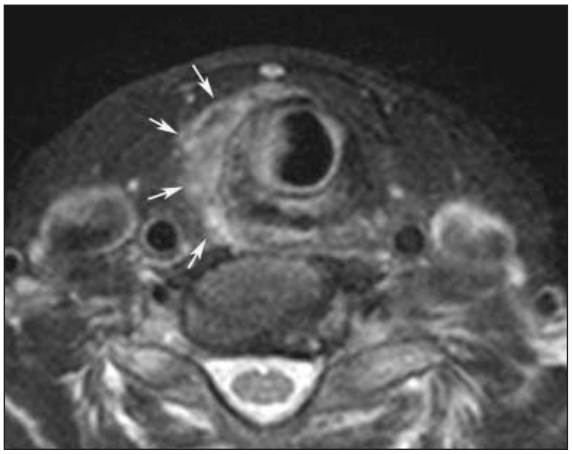

C

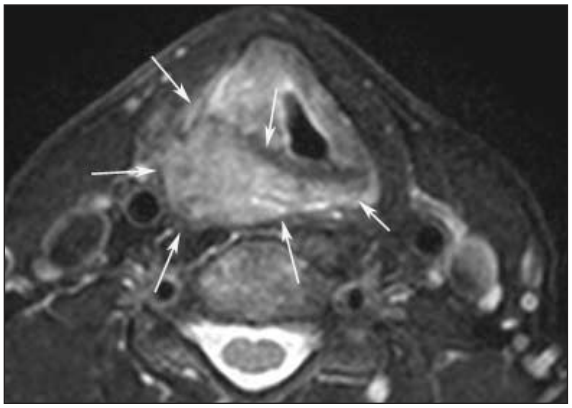

Figure 8. Hypopharyngeal squamous cell carcinoma in a 69-year-old man. **A**, Transverse gray scale sonogram shows a relatively well-defined hypoechoic mass (arrows) at the upper pole of the thyroid gland. **B**, Fat suppressed T2-weighted MRI shows a poorly defined hyperintense mass (arrows) at the upper pole of the right thyroid gland. **C**, Fat suppressed T2-weighted MRI shows a poorly defined hyperintense mass (arrows) at the right hypopharynx involving the right pyriform sinus. **D**, Gross specimen at the posterior aspect shows a lobulating mass (black arrows) arising from the right pyriform sinus (blue arrows indicate thyroid cartilage; and green arrows, false vocal fold). **E**, Pathologic specimen shows that the squamous cancer cells have invaded the cartilage (arrows; H&E, original magnification ×40).

D

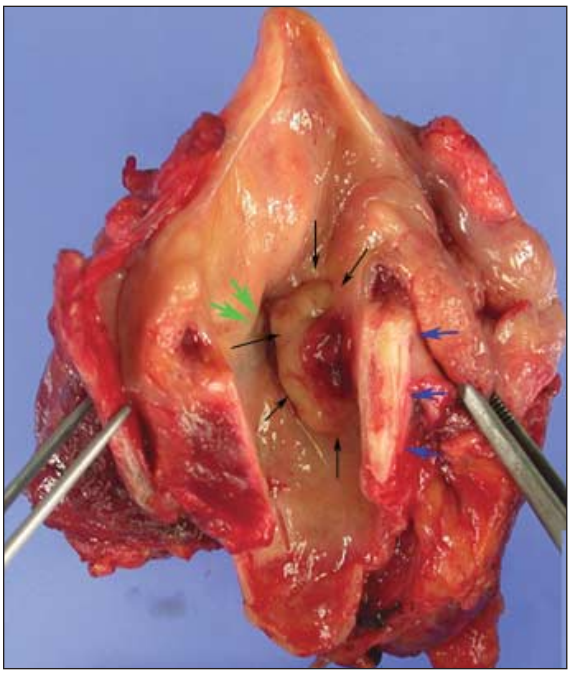

E

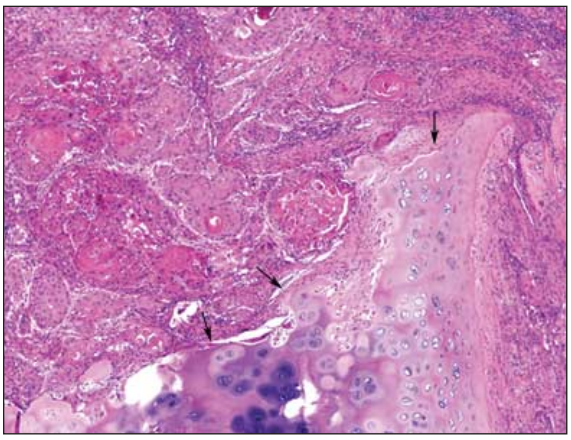

Sometimes a target sign can be seen in peripheral nerve sheath tumors, with a hypoechoic peripheral zone and a hyperechoic central zone on sonography.[24] A heterogeneous appearance with cystic degeneration is much more common in schwannoma than neurofibroma.[24] In this study, a peripheral nerve sheath tumor could be differentiated from a thyroid mass by the appearance of a well-demarcated mass separated from the thyroid gland and a mass effect of the adjacent thyroid gland from the tumor.

Figure 9. Tracheal adenoid cystic carcinoma in a 33-year-old woman. **A**, Transverse gray scale sonogram shows a well-defined hypoechoic mass (arrows) at the medial part of the right thyroid gland. **B**, Longitudinal gray scale sonogram shows a hypoechoic mass (arrows) at the posterior aspect of the thyroid gland. **C**, Contrast-enhanced coronal CT shows a well-defined hypodense soft tissue mass (arrows) in the inferomedial portion of the right thyroid gland, narrowing the mid trachea. **D**, Bronchography shows a smooth marginated elevated lesion (arrows).

A

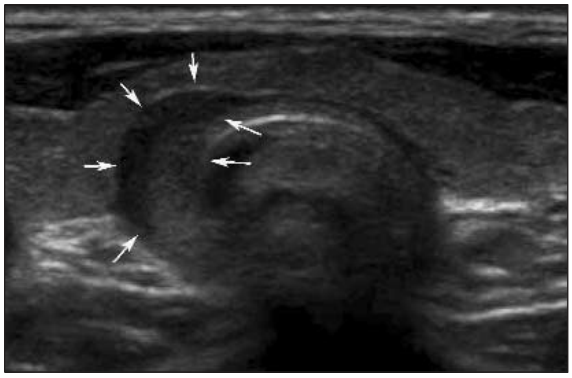

B

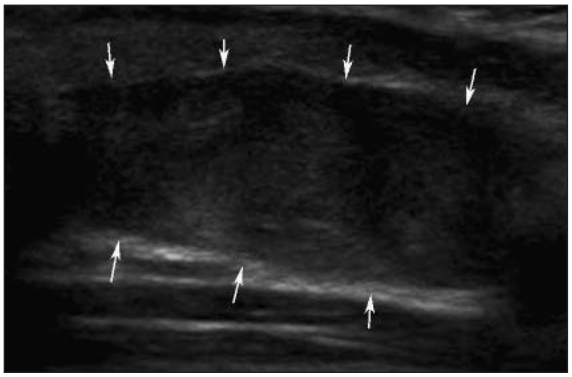

C

D

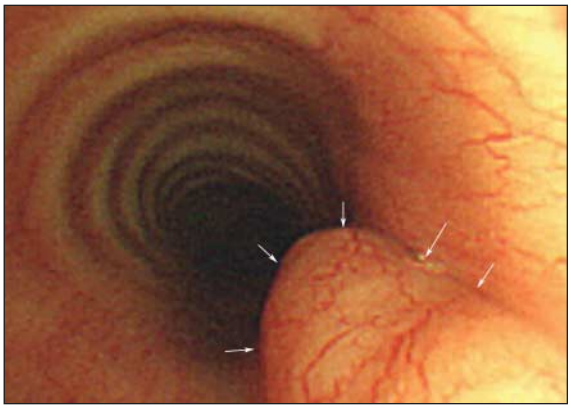

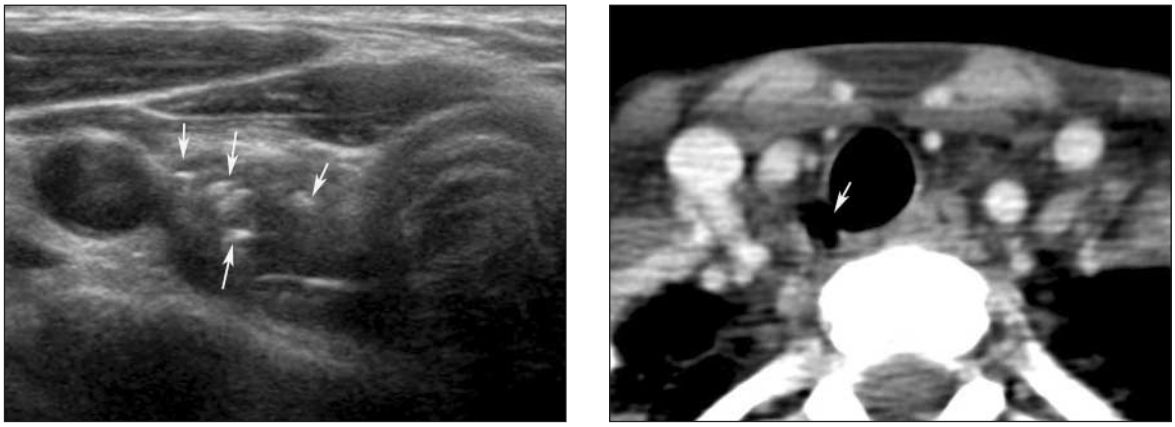

A B

Figure 10. Paratracheal air cyst in a 40-year-old woman. **A**, Transverse gray scale sonogram shows a well-defined hypoechoic mass with multiple hyperechoic dots (arrows) at the inferoposterior aspect of the right thyroid gland. **B**, Axial CT shows communication (arrow) between the trachea and the air cyst.

Conclusions

Radiologists should be aware of the various conditions that can affect the anterior neck surrounding the thyroid glands. To diagnose anterior neck lesions, sonography is the cornerstone for localizing, differentiating, and guiding biopsy. Although some of these disease processes may present as extrathyroid lesions on sonography, knowledge of the sonographic features of extrathyroidal lesions, a clinical history including laboratory findings, and aspiration or biopsy may be helpful in evaluation of some extrathyroid diseases by allowing for differentiation between thyroid and extrathyroid lesions. Therefore, an awareness of a wide range of extrathyroid lesions is important to avoid misdiagnosis and to help with further diagnostic evaluations.

Figure 11. Mediastinal teratoma in a 23-year-old woman. **A**, Transverse gray scale sonogram shows a huge nearly cystic mass (arrows) at the left thyroid gland. **B**, Contrast-enhanced axial CT shows a well-defined hypodense mass (arrows) at the left thyroid gland (continued).

A B

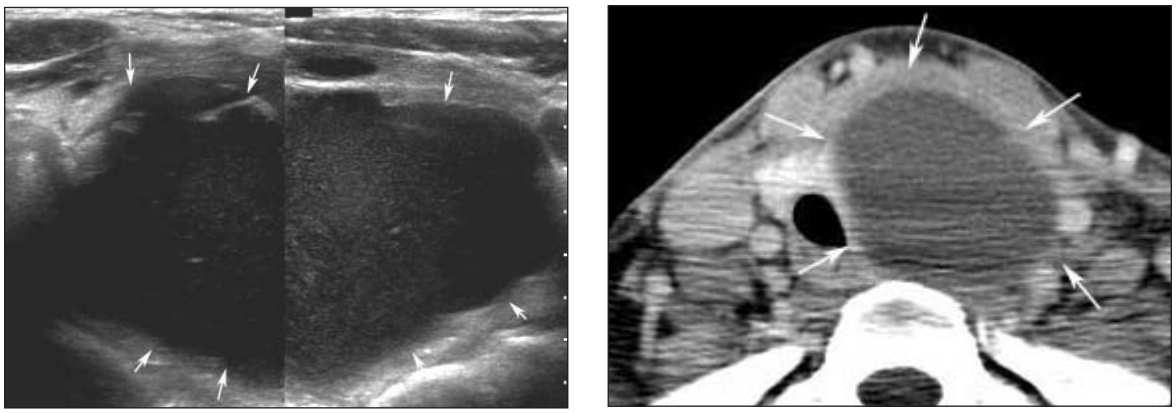

C

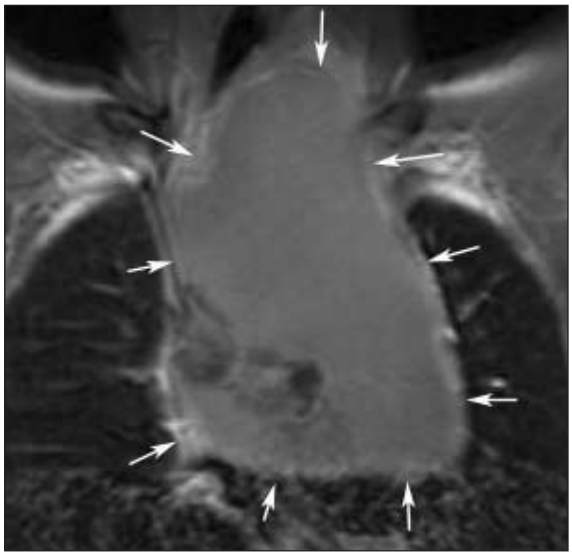

D

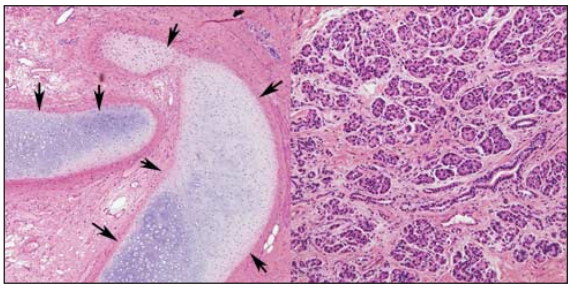

E

Figure 11. (continued) **C**, Contrast-enhanced axial CT shows a well-defined hypodense mass (white arrows) with an internal fat component (black arrow), suggesting teratoma in the anterior mediastinum. **D**, T1-weighted MRI shows a mediastinal mass (arrows) extending into the left neck. **E**, Pathologic specimen shows that the tumor is composed of mature cutaneous adnexa, cartilage (left, arrows; H&E, original magnification ×40), and pancreatic tissue (right; H&E, original magnification ×100).

Figure 12. Mediastinal lymphoma in a 23-year-old woman. **A** and **B**, Transverse gray scale sonograms show multiple conglomerated hypoechoic masses (arrows) at the inferoposterior aspect of the thyroid gland (continued).

A

B

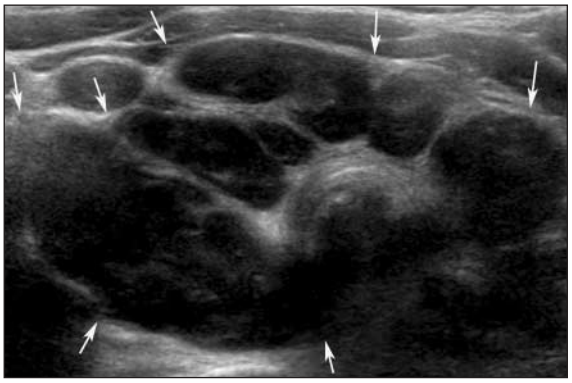

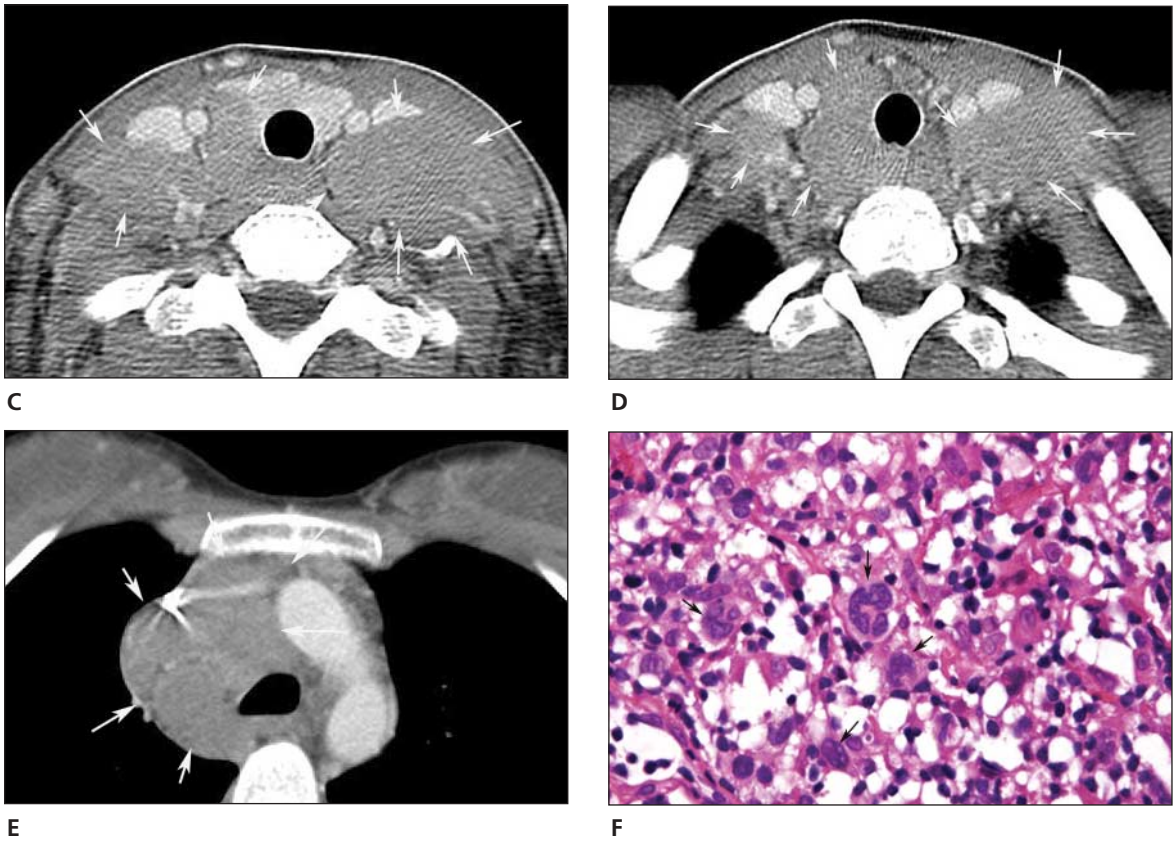

Figure 12. (continued). **C**–**E**, Contrast-enhanced axial CT shows multiple conglomerated hypodense masses (arrows) in the supero-posterior mediastinum, extending to the posterior aspect of the thyroid gland. **F**, Pathologic specimen shows that the lymph node architecture is effaced by various numbers of mononuclear Hodgkin cells and multinucleated Reed-Sternberg cells (arrows; H&E, original magnification ×400).

Figure 13. Desmoid tumor in a 36-year-old woman. **A**, Transverse gray scale sonogram shows a well-defined hypoechoic mass (arrows) at the posterior aspect of the left thyroid gland. **B**, Longitudinal gray scale sonogram shows a well-defined hypoechoic mass (arrows) at the inferior aspect of the right thyroid gland (continued).

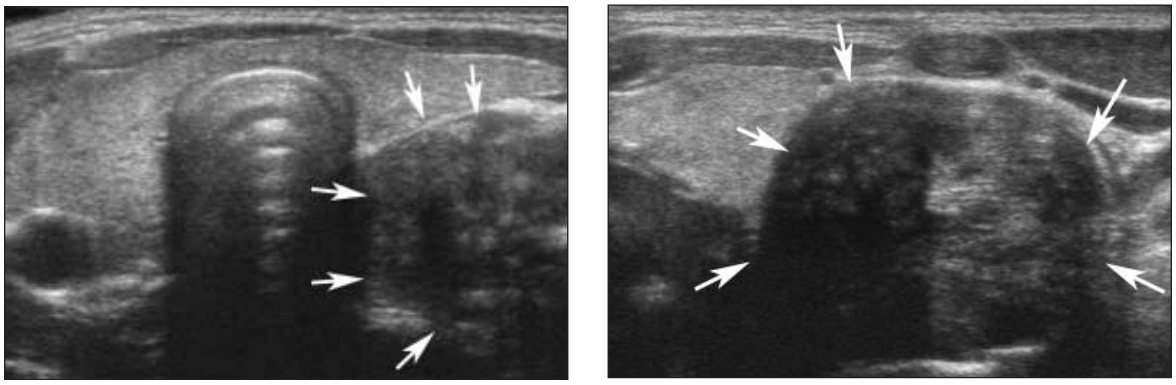

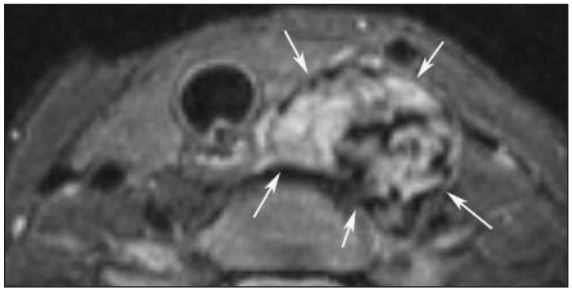

C

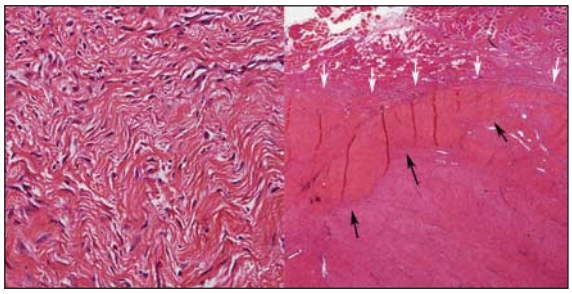

D

Figure 13. (continued). **C**, Fat-suppressed T2-weighted MRI shows a well-defined hyperintense mass with an internal hypodense area at the posterior aspect of the left thyroid gland (arrows). **D**, Pathologic specimen shows that the tumor is composed of palely eosinophlic fibroblasts and myofibroblasts with variably tapering or plump vesicular nuclei (left; H&E, original magnification ×200). The cellularity is variable within tumor (right, white arrows) and shows focal hyalinization (right, black arrows; H&E, original magnification ×200). At the advancing edge of the tumor, degenerated skeletal muscle cells are present.

Figure 14. Schwannoma in a 65-year-old woman. **A** and **B**, Transverse and longitudinal gray scale sonograms show a well-defined heterogeneous hypoechoic mass (arrows), compared with the adjacent thyroid tissue, between the left thyroid gland and the common carotid artery. **C**, Contrast-enhanced axial CT shows a well-defined hypodense mass (arrows) at the posterior aspect of the left thyroid gland. **D**, Pathologic specimen shows that the smear has several clusters of spindly cells (arrows) with variable cellularity and elongated wavy nuclei with a pale and fibrillar cytoplasm (H&E, original magnification ×400).

A

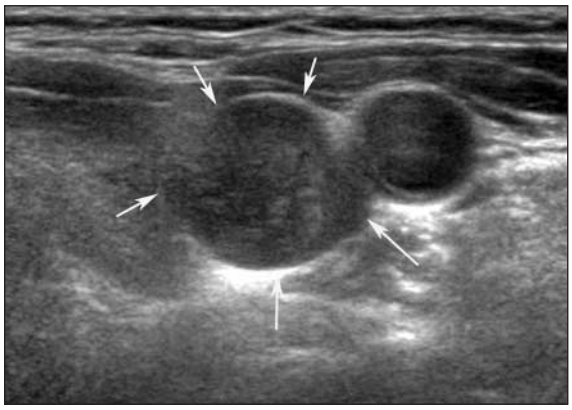

B

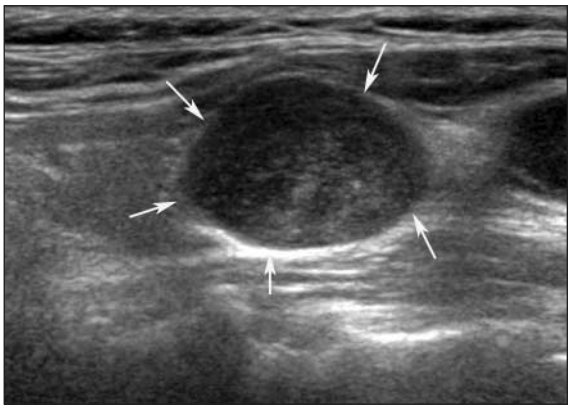

C

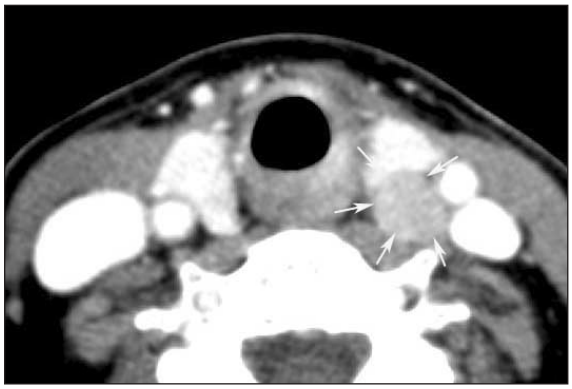

D

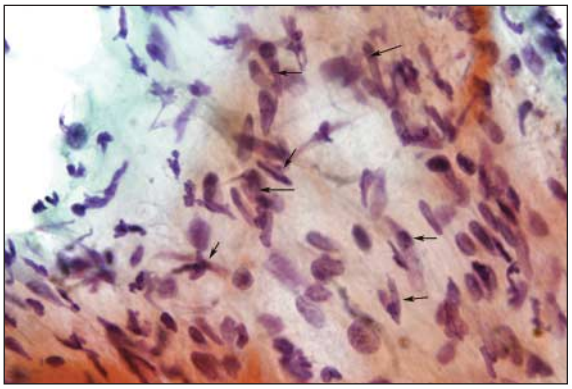

References

1. Akerström G, Malmaeus J, Bergström R. Surgical anatomy of human parathyroid glands. Surgery 1984; 95:14–21.
2. Kamaya A, Quon A, Jeffrey RB. Sonography of the abnormal parathyroid gland. Ultrasound Q 2006; 22:253–262.
3. Reeder SB, Desser TS, Weigel RJ, Jeffrey RB. Sonography in primary hyperparathyroidism: review with emphasis on scanning technique. J Ultrasound Med 2002; 21:539–552.
4. Rosario PW, de Faria S, Bicalho L, et al. Ultrasonographic differentiation between metastatic and benign lymph nodes in patients with papillary thyroid carcinoma. J Ultrasound Med 2005; 24:1385–1389.
5. Kumar A, Aggarwal S, Pham DH. Pharyngoesophageal (Zenker's) diverticulum mimicking thyroid nodule on ultrasonography: report of two cases. J Ultrasound Med 1994; 13:319–322.
6. Ekberg O, Nylander G. Lateral diverticula from the pharyngo-esophageal junction area. Radiology 1983; 146:117–122.
7. Kim J, Kim YJ, Kim EK, Park CS. Incidentally found pharyngoesophageal diverticulum on ultrasonography. Yonsei Med J 2002; 43:271–273.
8. Kwak JY, Kim EK. Sonographic findings of Zenker diverticula. J Ultrasound Med 2006; 25:639–642.
9. Biggi E, Derchi LE, Cicio GR, Neumaier CE. Sonographic findings of Zenker's diverticulum. J Clin Ultrasound 1982; 10:395–396.
10. Komatsu M, Komatsu T, Inove K. Ultrasonography of Zenker's diverticulum: special reference to differential diagnosis from thyroid nodules. Eur J Ultrasound 2000; 11: 123–125.
11. DeFriend DE, Dubbins PA. Sonographic demonstration of a pharyngoesophageal diverticulum. J Clin Ultrasound 2000; 28:485–487.
12. Livstone EM, Skinner DB. Tumors of the esophagus. In: Berk JE (ed). Gastroenterology. Philadelphia, PA: WB Saunders Co; 1985:818–850.
13. Som PM, Curtin HD. Trachea: anatomy and pathology. In: Sasson JP, Abdelrahman NG, Aquino S, Lev MH (eds). Head and Neck Imaging. 4th ed. St Louis, MO: CV Mosby Co; 2003:1700–1726.
14. Tanaka H, Mori Y, Kurokawa K, Abe S. Paratracheal air cysts communicating with the trachea: CT findings. J Thorac Imaging 1997; 12:38–40.
15. Goo JM, Im JG, Ahn JM, et al. Right paratracheal air cysts in the thoracic inlet: clinical and radiologic significance. AJR Am J Roentgenol 1999; 173:65–70.
16. Infante M, Mattavelli F, Valente M, Alloisio M, Preda F, Ravasi G. Tracheal diverticulum: a rare cause and consequence of chronic cough. Eur J Surg 1994; 160:315–316.
17. Tanaka H, Igarashi T, Teramoto S, Yoshida U, Abe S. Lymphoepithelial cysts in the mediastinum with an opening to the trachea. Respiration 1995; 62:110–113.
18. Kim YJ, Kim EK, Kim J, Park CS. Paratracheal air cysts: sonographic findings in two cases. Korean J Radiol 2003; 4:136–139.
19. Mountzios G, Pavlakis G, Terpos E, et al. Concurrent development of testicular seminoma and choriocarcinoma of the superior mediastinum, presented as cervical mass: a case report and implications about pathogenesis of germ-cell tumours. BMC Clin Pathol 2006; 6:8–14.
20. Alvarez ZC, Riveros SP, Miranda TR, Yarur VO. Mediastinal hydatid cyst: case report and review. Rev Chilena Infectol 2007; 24:149–152.
21. Tomà PL, Rossi UG. Paediatric ultrasound, II: other applications. Eur Radiol 2001; 11:2369–2398.
22. Gaerte SC, Meyer CA, Winer-Muram HT, Tarver RD, Conces DJ. Fat-containing lesions of the chest. Radiographics 2002; 22(special issue):S61–S78.
23. Dinauer PA, Brixey CJ, Moncur JT, Fanburg-Smith JC, Murphey MD. Pathologic and MR imaging features of benign fibrous soft-tissue tumors in adults. Radiographics 2007; 27:173–187.
24. Lin J, Martel W. Cross-sectional imaging of peripheral nerve sheath tumors: characteristic signs on CT, MR imaging, and sonography. AJR Am J Roentgenol 2001; 176:75–82.